Physica D 393 (2019) 38–46

Contents lists available at ScienceDirect

Physica D

journal homepage: www.elsevier.com/locate/physd

The effect of integral control in oscillatory and chaotic reaction kinetic networks

Kristian Thorsen [a,*], Tormod Drengstig [a], Peter Ruoff [b]

[a] Department of Electrical Engineering and Computer Science, University of Stavanger, Norway
[b] Centre for Organelle Research, University of Stavanger, Norway

HIGHLIGHTS

- Biological reaction kinetic networks can show oscillatory and chaotic behavior.
- We study the effect of integral control in systems that show oscillations.
- We show that integral control has a regulatory effect even during oscillations.
- We study the behavior of the Brusselator with and without added integral control.
- Integral action defends the average value in both periodic and chaotic oscillations.

ARTICLE INFO

Article history:
Received 6 May 2018
Received in revised form 14 January 2019
Accepted 17 January 2019
Available online 30 January 2019
Communicated by K. Josic

Keywords:
Reaction networks
Integral control
Chaos
Oscillations
Homeostasis

ABSTRACT

Integral control is ubiquitously used in industrial processes to keep variables robustly regulated at a given setpoint. Integral control is also present in many biological systems where it, implemented through reaction kinetic networks of genes, proteins and molecules, protects the organism against external variations. One difference between industrial control systems and organisms is that oscillatory behavior seems to be more common in biology. This is probably because engineers can choose to design systems that avoid oscillations. Looking at regulation from the viewpoint of biological systems, the prevalence of oscillations leads to a question which is not often asked in traditional control engineering: how can regulatory and adaptive mechanisms function and coexist with oscillations? And furthermore: does integral control provide some kind of robust regulation in oscillatory systems? Here we present an analysis of the effect of integral control in oscillatory systems. We study nonlinear reaction kinetic networks where integral control is internally present and how these systems behave for parameter values that produce periodic and chaotic oscillations. In addition, we also study how the behavior of an oscillatory reaction kinetic network, the Brusselator, changes when integral control is added to it. Our results show that integral control, when internally present, in an oscillatory system robustly defends the average level of a controlled variable. This is true for both periodic and chaotic oscillations. Although we use reaction kinetic networks in our study, the properties we find are applicable to all systems that contain integral control.

1. Introduction

From a control engineering point of view it is clear that negative feedback with integral control is an attractive mechanism for providing robust regulation. Integral control is also common in biology. Many studies have indeed identified integral control to be internally present in reaction kinetic networks of regulatory biochemical systems [1–4], and there is an ongoing effort in synthetic biology to design integral control motifs that can be used in engineered cells [5–7] . However, because of practical constraints and limitations, biological controllers do most often not operate with the same mathematical simplicity and purity as man-made controllers in electromechanical systems [5–9].

Although the theory behind integral control is well established, not much work has been done on its effect in oscillatory systems. This may be because oscillations are traditionally avoided in man made control systems. It is relatively straightforward to design systems that do not oscillate, so why consider systems that do?

There are many biochemical systems that display oscillatory behavior [10,11]. Examples include metabolic glycolysis [12,13], circadian rhythms [14,15], and synthetic genetic networks [16–19]. Oscillatory behavior is also observed in pure chemical reactions like the Belousov–Zhabotinskii reaction [20,21]. This reaction is often studied as a model for more complex biochemical

* Corresponding author.
E-mail address: kristian.thorsen@uis.no (K. Thorsen).

https://doi.org/10.1016/j.physd.2019.01.002

processes, for instance in relation to synchronization of oscillations across unicellular populations [22,23]. Most of the oscillatory systems in biology show periodic oscillations, but there are also systems that show irregular and chaotic oscillations under specific conditions [13,24,25]. Such chaotic behavior is seen in chemical oscillators [26,27], enzyme-catalyzed reactions [28,29], excitable cells [30,31], and in glycolysis [32,33]. In addition to experimental observations chaos has also been shown to exist in mathematical models of metabolic networks, for example in a model of glycolysis [33], and in a model of metabolism and redox balance in mitochondria [34].

In this work we study integral control in reaction kinetic networks and focus on regulation from the viewpoint of biochemical systems. The properties we find should however be generally applicable to all systems that contain integral control.

1.1. Integral control in reaction kinetic networks

We have previously presented a set of simple two component network motifs with structures that can provide integral control [4,35]. Two such motifs are used in this study to examine how integral control affects oscillatory networks. An outflow controller (type 5 in [4]) is used here in the main text, and an inflow controller (type 2 in [4]) is used in the Supplementary Material (SM). The outflow controller is shown in Fig. 1a; the solid lines represent mass flow, and the dashed lines represent signaling. A chemical species A, called the controlled species, is regulated through negative feedback by a chemical species E, called the controller species. The controller species compensates for changes in A, caused by disturbance in the inflow (or outflow) of A, by adjusting a compensatory outflow $j = k_3AE/(K_M^A+A)$. The motif is called an outflow controller because it adjusts an outflow.

The change in E is described by the following rate equation

$$\dot{E} = k_5A - \frac{k_6E}{K_M^E + E}, \tag{1}$$

where the removal of E is described by a Michaelis–Menten expression. Integral control is most easily implemented by having zero-order removal of E with respect to itself, but other arrangements are also possible [36]. Assuming zero-order removal (saturation with $K_M^E \ll E$) the rate equation for E becomes

$$\dot{E} = -k_5\left(\frac{k_6}{k_5} - A\right), \tag{2}$$

which is similar to the standard integral control law [35]. The equation for $\dot{E}$ has A as its only variable, that is: $\dot{E} = h(A)$. The steady state condition, $h(A) = 0$, gives a simple expression for the defended level of A (the setpoint):

$$A_{set} = \frac{k_6}{k_5}. \tag{3}$$

The function of this controller motif can be illustrated by the block schematic representation in Fig. 1b. This representation, which is commonly used in control engineering, shows that the concentration of the controller E is the integrated difference (error) between the setpoint and the fed back measurement of A.

2. Methods

We will use two different approaches to examine the effect of integral control in oscillatory reaction kinetic networks. The first approach (in Sections 3.1 and 3.2) is to use a reaction kinetic network where integral control is already present, i.e., the controller motif from Fig. 1a, and extend/alter this network until oscillatory behavior appears. The second approach (in Section 3.3) is to add integral control to an already oscillating system. For this

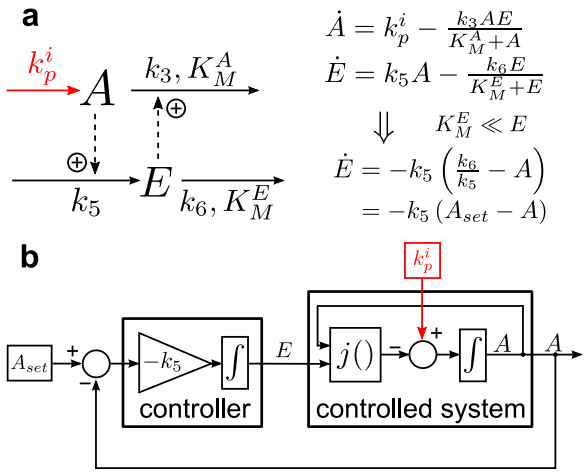

Fig. 1. Negative feedback outflow controller. (a) Reaction network representation and rate equations for the motif. The controller variable E is activated by A and feeds back by adjusting the outflow of A. We treat a changing inflow of A through the parameter k_p^i as the primary disturbance to the system, see the text under Section 2 Methods. (b) Control engineering type block schematic representation showing how the motif can be separated into a controller and a controlled system. The primary disturbance (k_p^i) is marked in red. The $j()$ block represents how the controller (E) affects the controlled system (A), i.e., by a compensatory flow $j = k_3AE/(K_M^A + A)$.

we will use the oscillatory reaction kinetic network known as the Brusselator [37,38] and add integral control in form of only the E-part from a controller motif, i.e., add Eq. (1) and an E-dependent outflow of the variable to be controlled.

The first approach can be thought of as similar to how oscillatory behavior may develop in existing regulatory reaction kinetic networks in cells and organisms, either through evolution, or through internal changes within a single organism. The second approach is more an engineer's approach where one has a system and then adds something to the system to see how it alters behavior. Since the system already oscillates this method makes it possible to see how the oscillatory behavior differs with and without integral control in the system.

We will throughout the work presented here use integral control motifs that act on the outflow of the species to be controlled. This is similar to an industrial controller that controls the level in a water tank by controlling an actuator in the form of an outflow valve or an outflow pump. In other words, the actuator removes the controlled species, called A, from the system when it is in excess. Since the actuator is unable to add A to the system, i.e., provide a negative outflow, it is most suited to compensate for disturbances in the inflow to the system. We will thus treat parameters that change the inflow of A as the main disturbances to the system.

Note that the situation is opposite for a reaction kinetic system where integral control is provided by an inflow controller motif (see SM6). A controller that compensates by adjusting an inflow is best suited to compensate against changes in outflow, i.e., disturbances in outflow. For a more detailed discussion about the differences between inflow and outflow controller motifs, what type of disturbances they are suited to compensate for, and what happens when disturbances that they are not fitted to compensate against start to dominate, we refer to our previous work in [4,39].

Computations were performed by using Matlab (mathworks.com). Numerical integrations were done with the variable step stiff solver *ode15s* (supplied with Matlab). A relative tolerance of 10^{-9}, an absolute tolerance of 10^{-12}, and a maximum step size of 0.1 was specified as solver options. State variables (A, E, Z, etc.) will typically represent concentrations of chemical compounds.

The word equilibrium point is herein used to describe a constant solution to a system of differential equations, i.e., a point where $\dot{x}_i = 0$ for all i state variables.

2.1. A note on degree of perfectness

The term setpoint is herein used as the theoretical steady state value of A given perfect zero-order removal of E in the above controller motifs. In other words, under pure and perfect integral control. The removal will however never be exactly zero-order in real biochemical networks, i.e., K_M^E will have a value different from zero. This will shift the actual stationary value of a controller motif away from the theoretical setpoint. The difference between the setpoint and the actual stationary value is a measure of the controller's accuracy [4], or better put inaccuracy [39], and it is related to the value of the fraction $f(E)$ given as:

$$f(E) = \frac{E}{K_M^E + E}. \tag{4}$$

This fraction represents the degree of zero order removal of E, and thus the degree of perfect integral control. To exemplify, consider a stationary case where $E = 10$ and $K_M^E = 0.1$. Then $f(E) \approx 1$ and we have tight control (small inaccuracy). In another situation where $E = 0.4$ and $K_M^E = 0.1$, we get $f(E) = 0.8$ implying 20% deviation between A and A_{set}.

This inaccuracy can be almost impossible to detect if very low K_M^E values like 10^{-6} are used. We have in this study selected to use K_M^E values that make the effect visible. See [4,40] for more details.

3. Results

We start the first approach with a motif that already contains integral control. The presented controller motif from Fig. 1a, and the rest of the complete set of motifs [4], can be extended to create systems that show sustained oscillations [41]. Such extensions can be done without changing the structure of the controller part (E), leaving a functional integral controller in the oscillating system.

3.1. Control of average concentration during periodic oscillations

Consider an oscillatory version of the outflow controller with added autocatalysis, shown in Fig. 2a. The equation for change in E is the same as before (Eq. (1)), but the change in A is now described by:

$$\dot{A} = k_p^i + k_2 A - \frac{k_3 A E}{K_M^A + A}. \tag{5}$$

The rate constant k_p^i is still the inflow disturbance and k_2 is the autocatalytic part. This motif oscillates for a wide range of parameter values. Stronger autocatalysis (higher k_2) leads to oscillations with greater amplitude. Fig. 2b shows a bifurcation diagram of how the amplitude of the oscillations in A changes with the strength of autocatalysis.

Examples of the behavior in A and E for a stepwise change in k_p^i are shown in Fig. 3a and b. Interestingly the average of A, denoted $\langle A \rangle$ (black line in Fig. 3a), seems to be only transiently affected by the disturbance. We did several similar simulations/experiments to this and to other oscillating controller motifs, and they all indicated the same: The average level of A appears to be regulated. The results of a full sweep study of the average level of A versus the strength of inflow disturbance for this outflow motif are shown in Fig. S1 in SM1.

The general property of integral control, that a controller regulates A to a setpoint, is derived from the steady-state condition, $\dot{E} = h(A) = 0$. The steady-state condition can however not be used when the controllers are oscillating.

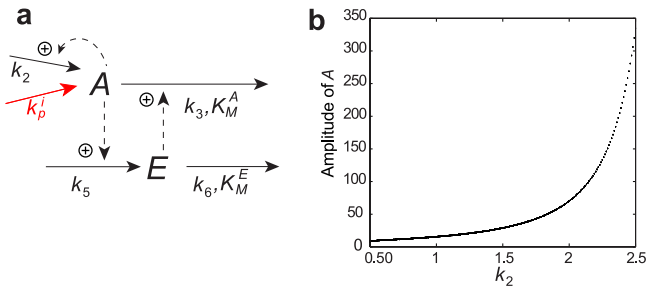

Fig. 2. A negative feedback outflow controller with oscillatory behavior. (a) Outflow controller with autocatalysis in A (Eqs. (5) and (1)). The controller variable E is activated by A and feeds back by adjusting the outflow of A. We treat a changing inflow of A, the parameter k_p^i, as the primary disturbance to the system. (b) Bifurcation diagram showing how the amplitude of the oscillations in A changes with the strength of autocatalysis k_2. Parameters: k_p^i=4, k_3=3.8, k_5=0.65, k_6=5.4, K_M^A=0.15, and K_M^E=0.5. Initial conditions: A_0=25.95, E_0=7.63.

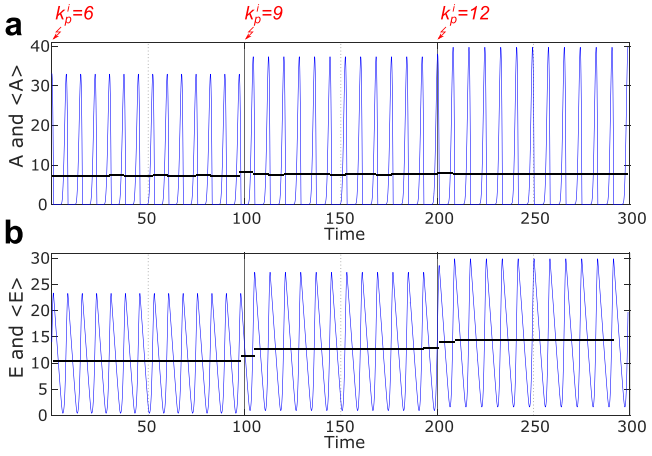

Fig. 3. Response to inflow disturbance changes in an oscillatory outflow controller. (a) Oscillations in A shown for a stepwise inflow disturbance in k_p^i from 6 to 9 at t=100, and from 9 to 12 at t=200, as indicated. The black line shows the periodic average of A, calculated between peaks. Parameters: k_2=1.5, k_3=3.8, k_5=0.65, k_6=5.4, K_M^A=0.15, and K_M^E=0.5. Initial conditions: A_0=33, E_0=14. (b) Oscillations in and average of E during the same disturbance.

In order to derive the property of integral control during periodic oscillations we start by the definition of periodicity. For each repeating cycle E is back at exactly the same value

$$E(t + T) = E(t), \tag{6}$$

where T is the *period time*, the time of one cycle. The change in E cannot be assumed to be zero, as in nonoscillatory systems (steady state condition), but the integrated change in E over one period must be zero:

$$\int_t^{t+T} \dot{E}\, dt = E(t + T) - E(t) = 0. \tag{7}$$

This must also be the case for any integer number n of periods from t to $t + nT$. We now introduce the *periodic average* value of $\dot{E}$, denoted $\langle \dot{E} \rangle$, which must also be zero:

$$\langle \dot{E} \rangle \triangleq \frac{1}{T} \int_t^{t+T} \dot{E}\, dt = 0. \tag{8}$$

The rate equation of E for any motif can be inserted into Eq. (8). Inserting $\dot{E}$ from Eq. (1) into Eq. (8) gives:

$$\langle \dot{E} \rangle = \frac{1}{T} \int_t^{t+T} \left(k_5 A - \frac{k_6 E}{K_M^E + E} \right) dt. \tag{9}$$

By applying zero-order kinetics, i.e., $K_M^E \to 0$, this reduces to

$$\langle \dot{E} \rangle = k_5 \left(\frac{1}{T} \int_t^{t+T} A\, dt \right) - k_6 \left(\frac{1}{T} \int_t^{t+T} 1\, dt \right) \tag{10}$$

$$= k_5 \left(\frac{1}{T} \int_t^{t+T} A\, dt \right) - k_6, \tag{11}$$

where the periodic average of A, denoted $\langle A \rangle$ can be identified. Using this and $\langle \dot{E} \rangle = 0$ (Eq. (8)) we find that the controller maintains the periodic average of A at a setpoint which we term $\langle A \rangle_{set}$:

$$\langle A \rangle \triangleq \frac{1}{T} \int_t^{t+T} A\, dt = \frac{k_6}{k_5} = \langle A \rangle_{set}. \tag{12}$$

Note that this derivation also holds for nonoscillatory controller motifs. A system in steady state is a trivial solution of Eq. (6).

Similar to the stationary case (Eq. (3)), the setpoint $\langle A \rangle_{set}$ in Eq. (12) is a theoretical setpoint that depends on $K_M^E \to 0$. The actual average $\langle A \rangle$ may thus differ somewhat from $\langle A \rangle_{set}$ at realistic conditions when K_M^E has a nonzero value (see Section 2.1).

3.2. Controller action in the chaotic regime

We will in this section extend our results and look into the function of integral control in systems with sustained nonperiodic oscillations. To do this we will first show how systems based on the presented controller motifs can be extended from periodic to chaotic oscillating systems.

In systems of ordinary differential equations chaos can only appear if the system has a dimension of three or higher and only if at least one of the equations is nonlinear. These conditions do not, however, guarantee the presence of a chaotic solution. Even if we do not know all the necessary and sufficient conditions for chaos, the composition of chaotic systems in three dimensions is relatively well known [42,43].

One way to build a system which should be able to show chaos, at least for some parameter values, is to combine a two dimensional oscillator with a switch; a type of structure first conceived by O. Rössler in some of the earliest studies of chaotic systems [44, 45]. The idea is best explained by the behavior in phase space. A trajectory spirals outwards from an unstable focus towards where the oscillator in two dimension would have formed an attractive limit cycle. Somewhere on this path the switch is activated and it lifts the trajectory up and into an area in phase space where the flow is reversed. The trajectory is then brought back down closer to the unstable focus than it was before it was lifted out. This is called *reinjection* [43,44]. For this to work the state variable defining the switch should have comparably fast dynamics, so that it creates a manifold in phase space that guides the movement of the other two oscillating state variables.

With this in mind we expanded the oscillating outflow controller (Fig. 2a) with an extra state variable Z that acts as a single threshold switch. The reaction kinetic structure is shown in Fig. 4a where the original oscillating structure is colored in green and the new addition is colored in blue. The rate equations for this new motif are:

$$\dot{A} = k_p^i + k_2 A - \frac{k_3 A E}{K_{M,1}^A + A} - \frac{k_4 A Z}{K_{M,2}^A + A} \tag{13}$$

$$\dot{E} = k_5 A - \frac{k_6 E}{K_M^E + E} \tag{14}$$

$$\dot{Z} = k_7 A - \frac{k_8 Z}{K_M^Z + Z}. \tag{15}$$

The equation for Z is similar to E and is really just an extra negative feedback and outflow controller on A, but its dynamics is faster with relative high values on rate constants k_7 and k_8.

The surface created by the fast dynamics of Z divides the phase space into two regions, shown in Fig. 4b. The surface is given by

$$F_Z(A, E, Z) = k_7 A - \frac{k_8 Z}{K_M^Z + Z} = 0. \tag{16}$$

Fig. 4b also illustrates how this system, for a certain set of parameters, shows reinjection. A trajectory starts to move on the horizontal part of the surface without much change in Z. When the oscillations cause the value of A to rise above a threshold at around $A = 10$ the switch is activated and the trajectory is lifted upwards in phase space by an increasing Z; the trajectory is guided by the manifold. As Z increases $\dot{A}$ is reduced (Eq. (13)). Ultimately $\dot{A}$ turns negative and we have reversed flow compared to the lower part of phase space. As A is reduced so is Z and the trajectory is reinjected into the horizontal part of the surface. This then repeats before the trajectory again starts to move on the horizontal part of the surface, only somewhat closer to the focus which it oscillates around. This behavior continues indefinitely; the trajectory moves on a chaotic attractor as shown in Fig. 4c. A more detailed view of the direction of flow is given in Fig. S2 in SM2.

Whether the system displays this chaotic behavior or more simple periodic oscillations is dependent on the parameter values. As noted we are mainly interested in changes in behavior due to changes in inflow, and will thus focus on how the system responds to changes in the strength of autocatalysis k_2 and the disturbance k_p^i.

Fig. 4d shows a bifurcation diagram for the amplitude of A for an increasing inflow disturbance, k_p^i, and Fig. 4e shows the same for increasing autocatalysis k_2. These bifurcation diagrams reveal the characteristic period doubling route to chaos. Further studies of the chaotic attractor for this system, including Poincaré sections, first-return maps, and a movie or the movement of the attractor in phase space, are given in SM3.

The interesting questions are now: What happens with the average level of A during chaos? Will the integral action in E still provide robustness against disturbances in inflow? We first examined this by simulating the chaotic system for a range of different disturbances, and studied how the average level of A was affected. Before presenting the results we note that the definition of a periodic average $\langle A \rangle$ from Eq. (12) is not useful for chaotic systems since there is no defined period T. Instead of calculating the periodic average, we have calculated the average over a sufficiently long length of time τ as:

$$\langle A \rangle_\tau \triangleq \frac{1}{\tau} \int_{t_0}^{t_0+\tau} A\, dt. \tag{17}$$

The results from many simulations with k_p^i in the range from 4 to 40 are combined in Fig. 5, which shows the average level of A and E. We have here used $\tau = 50$ (what makes a sufficiently long τ is discussed towards the end of this section). The results indicate that the average level of A is still defended and that the presence of chaos does not alter the regulatory properties of the system. The average level of the controller species E increases with the level of the k_p^i disturbance. This makes sense from the structure of the reaction kinetic network, Fig. 4a; an increased inflow of A through k_p^i is compensated by an increased E-mediated outflow of A.

The response to stepwise changes in inflow disturbance (k_p^i) is shown in Fig. 6. The system is challenged with a step in k_p^i from a periodic region ($k_p^i = 13$) to a chaotic region ($k_p^i = 15$), and the controller responds by increasing the average level of E, which again increases the compensatory outflow of A. Fig. 6 also shows the response to a further step in the disturbance from $k_p^i = 15$ to $k_p^i = 20$.

Consequently, the integral controller E maintains the average level of A near the theoretical setpoint, as shown in Fig. 5. The

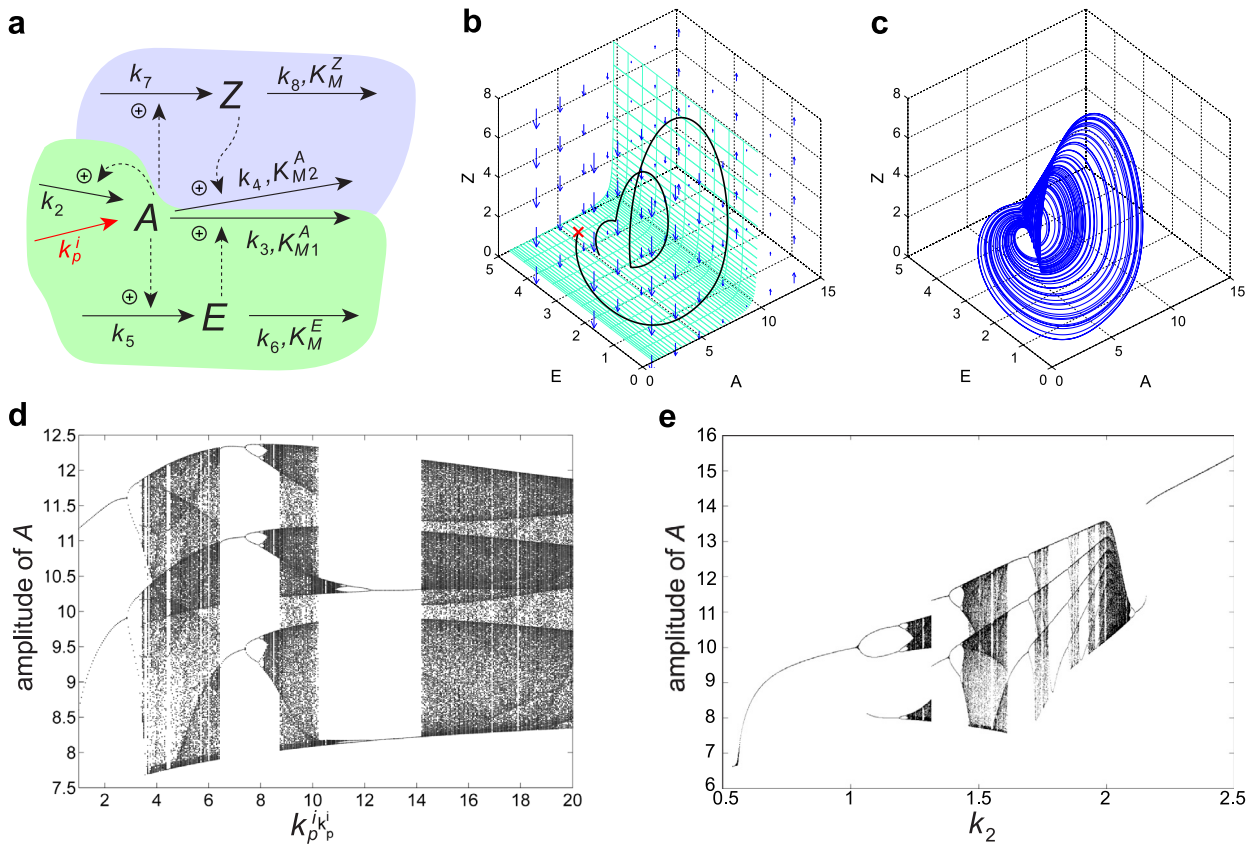

Fig. 4. Extended outflow controller capable of showing chaotic behavior. (a) Chaotic outflow controller built by combining an oscillating controller (green, identical to Fig. 2a) with a switch (blue, made out of a negative feedback similar to the controller structure, but with faster dynamics). (b) Phase space with the manifold created by the fast dynamics of the Z-switch (given by Eq. (16)). Blue arrows show the vector field of Z. A trajectory (in black) spiraling outwards from a focus point is reinjected, enabling the occurrence of chaos. Parameters: $k_p^i = 4$, k_2=1.5, k_3=3.8, k_4=3.7, k_5=0.65, k_6=5.4, k_7=7.7, k_8=75, $K^A_{M,1}$=$K^A_{M,2}$=0.15, K^E_M=0.5, and K^Z_M=0.03. The trajectory starts in [5.5, 4.5, 0.04] (red cross). (c) The chaotic attractor for this system shown in phase space. (d) Bifurcation diagram showing how the amplitude of the oscillations in A changes with disturbance in inflow k_p^i (other parameters as above). (e) Bifurcation diagram showing how the amplitude of the oscillations in A changes with the strength of the autocatalysis k_2 (other parameters as above). Simulations in (d) and (e) are run for 500 time units before collection of data to avoid transients. (For interpretation of the references to color in this figure legend, the reader is referred to the web version of this article.)

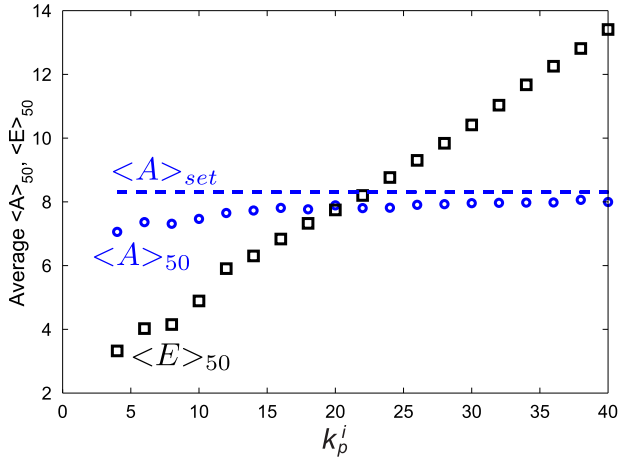

Fig. 5. Control of the average of A under chaotic conditions. (a) Average level of A, $\langle A\rangle_{50}$ (blue circles), for the chaotic outflow controller in Fig. 4a (Eqs. (13)–(15)) for different levels of inflow disturbances. The black squares show the average level of E, and the dashed blue line shows the theoretical setpoint of A, $\langle A\rangle_{set} = k_6/k_5$=8.3. The averages are calculated over a time length of τ=50. Parameters: k_2=1.5, k_3=3.8, k_4=3.7, k_5=0.65, k_6=5.4, k_7=7.7, k_8=75, $K^A_{M,1}$=$K^A_{M,2}$=0.15, K^E_M=0.5, and K^Z_M=0.03. Initial conditions: A_0=8.30, E_0=3.18 and Z_0=0.16. Transient effects are avoided by letting simulations run for a time length of 100 before starting the calculation of averages.

average value of A is maintained even though the system moves in and out of chaotic behavior as the inflow disturbance changes. The system changes between chaotic and periodic behavior as indicated in the bifurcation diagram in Fig. 4d. The small difference between $\langle A\rangle_\tau$ and the theoretical setpoint can be attributed to the level of E and the parameter K^E_M. Higher level of E means that its removal becomes more saturated, hence the $f(E)$ fraction (Eq. (4)) is closer to 1 and the controller becomes more accurate, see also Section 2.1.

Analytically deriving the properties of integral control during chaotic conditions may not seem as straightforward as in the periodic case. We can no longer use periodicity as we did in Eqs. (6)–(12). The integrated change of E from a point in time t_0 to a point in time $t_0+\tau$ will for an arbitrary value of τ be equal to some number ϵ, which is the difference between $E(t_0+\tau)$ and $E(t_0)$. That is:

$$\int_{t_0}^{t_0+\tau} \dot{E}\, dt = E(t_0+\tau) - E(t_0) = \epsilon. \tag{18}$$

For a system with a chaotic attractor we have that ϵ is bounded when $\tau \to \infty$, given that the trajectory is on the attractor at time t_0 (transients have died out). A trajectory already on a chaotic attractor (after transients) will forever move on the attractor, and thus $E(t_0+\tau)$ cannot move further away from $E(t_0)$ than the extent of the attractor along the E-axis in phase space.

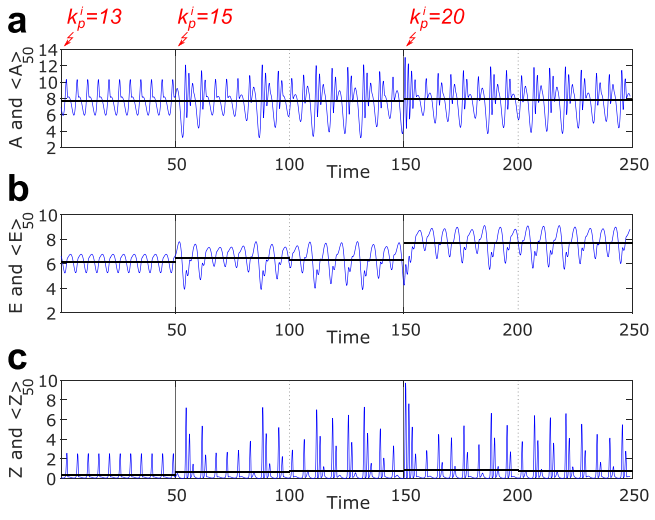

Fig. 6. Example response for the chaotic outflow controller to a stepwise change in inflow. (a) Response to an inflow disturbance given as a stepwise change for the chaotic outflow controller in Fig. 4a (Eqs. (13)–(15)). The disturbance k_p^i is stepped from 13 to 15 at t=50, and from 15 to 20 at t=150, as indicated. The level of A is shown in blue while the average of A, $\langle A\rangle_{50}$, is shown in black. (b) Level and average of E. (c) Level and average of Z. Parameters: k_2=1.5, k_3=3.8, k_4=3.7, k_5=0.65, k_6=5.4, k_7=7.7, k_8=75, $K_{M,1}^A$=$K_{M,2}^A$=0.15, K_M^E=0.5, and K_M^Z=0.03. Initial conditions: A_0=6.91, E_0=6.65 and Z_0=0.07. The averages are calculated over fixed intervals with a length of τ=50 starting from t=0 to t=50, from t=50 to t=100, and so on.

Taking the time average of $\dot{E}$ as in Eq. (17) we have that:

$$\langle E\rangle_\tau = \frac{1}{\tau}\int_{t_0}^{t_0+\tau} \dot{E}\,dt = \frac{\epsilon}{\tau}. \tag{19}$$

By continuing the derivation as in Eqs. (8)–(12) we find that integral control (implemented by zero-order kinetics) defends the average level of the controlled variable A at:

$$\langle A\rangle_\tau = \frac{1}{\tau}\int_{t_0}^{t_0+\tau} A\,dt = \frac{k_6}{k_5} + \frac{\epsilon}{k_5\tau}. \tag{20}$$

Furthermore when $\tau \to \infty$, this reduces to the same theoretical setpoint as in the periodic case (Eq. (12)), that is:

$$\lim_{\tau\to\infty} \langle A\rangle_\tau = \frac{k_6}{k_5} = \langle A\rangle_{set}. \tag{21}$$

This proves that integral control provides robust regulation even when the system behaves chaotically.

In practice τ does not have to go to infinity; it is sufficient to have τ large enough to make the contribution from ϵ negligible. From our experience it is enough to have a τ value that allows the trajectory to cover most of the attractor. Around 10 times the quasi-period, or 10 times around the attractor, is usually sufficient.

It is possible to relate the setpoint of $\langle A\rangle_\tau$ and the behavior of $\langle E\rangle_\tau$ seen in Fig. 5 to an unstable equilibrium point of the overall system. This is shown in SM4 and discussed further in the next section where we add integral control to an already oscillating system.

The above method for calculating the average of a variable is convenient as it works well for stationary, periodic, and chaotic behavior without much need for prior information about how the system behaves or the shape and position of the attractor in phase space. An alternative approach that is arguably more mathematical elegant, and equivalent to the periodic average, is to calculate the average between two successive intersections with a Poincaré section. This method is used in SM5 to calculate the averages during a change in inflow disturbance in the chaotic outflow controller (the same experiment as in Fig. 6), and the method gives similar results. However elegant, this method is more cumbersome as it requires prior information about the attractor in order to choose a fitting placement of the Poincaré section.

3.3. Adding integral control to an already oscillating reaction kinetic network

In the preceding parts we started with a reaction kinetic network that already contained an integral controller, and extended this system to show its behavior under periodic and chaotic oscillations. We will now take a different approach by starting with an oscillatory reaction kinetic network that does not contain integral control, and study how its behavior changes when integral control is added to the system.

The Brusselator is a widely studied theoretical reaction kinetic network that shows limit cycle oscillations. It was proposed by Lefever, Nicolis and Prigogine and is named after the city of Brussels where they were based [37,38]. The Brusselator can be expressed with two chemical species, X and Y, having the following rate equations [38,46]:

$$\dot{X} = k_p^i - k_2X + k_3X^2Y - k_4X \tag{22}$$

$$\dot{Y} = k_2X - k_3X^2Y. \tag{23}$$

A reaction network representation of the Brusselator is shown in Fig. 7a (do not consider the green part yet). To illustrate the effect of integral control we have selected to treat the independent inflow of X as a disturbance to the system, i.e., we let the rate constant k_p^i vary. The Brusselator system has *one* equilibrium point,

$$X^* = \frac{k_p^i}{k_4}, \quad Y^* = \frac{k_2k_4}{k_p^ik_3}, \tag{24}$$

that may be stable or unstable depending on the value of the rate constants. When the equilibrium is unstable the system has a stable limit cycle that gives rise to periodic oscillations. Note that the equilibrium value of X is dependent on the amount of inflow of X through the reaction described by the disturbance k_p^i.

The goal here is not to give a thorough examination of the stability and behavior of the Brusselator, which has been done elsewhere [38,46–48], but to look at how its behavior changes when an integral controller is added to the system.

The response of the Brusselator to stepwise changes in the disturbance k_p^i is shown in Fig. 7b and c. For the parameter values that we use (listed in the caption of Fig. 7) we see that the Brusselator is stable and that there are steady state solutions for $k_p^i = 0.5$ and $k_p^i = 0.3$. The Brusselator starts to oscillate when k_p^i is stepped from 0.3 to 0.25. The simulation results show that the value of X (and Y) during steady state and the periodic average $\langle X\rangle$ (and $\langle Y\rangle$) during oscillations change with varying disturbance values, as expected from Eq. (24).

Consider now that we want to control the (average) value of X in the Brusselator by adding an integral controller in the form of the controller motif marked with green in Fig. 7a. The extended equations for this controlled Brusselator are:

$$\dot{X} = k_p^i - k_2X + k_3X^2Y - k_4X - k_7XE \tag{25}$$

$$\dot{Y} = k_2X - k_3X^2Y \tag{26}$$

$$\dot{E} = k_5X - \frac{k_6E}{K_M^E + E}. \tag{27}$$

The key point now is that the integral controller changes the equilibrium value of X, making it independent of the parameters in the original Brusselator. As in Eqs. (3), (12), and (21) the controller introduces a setpoint for X at k_6/k_5, which is only dependent

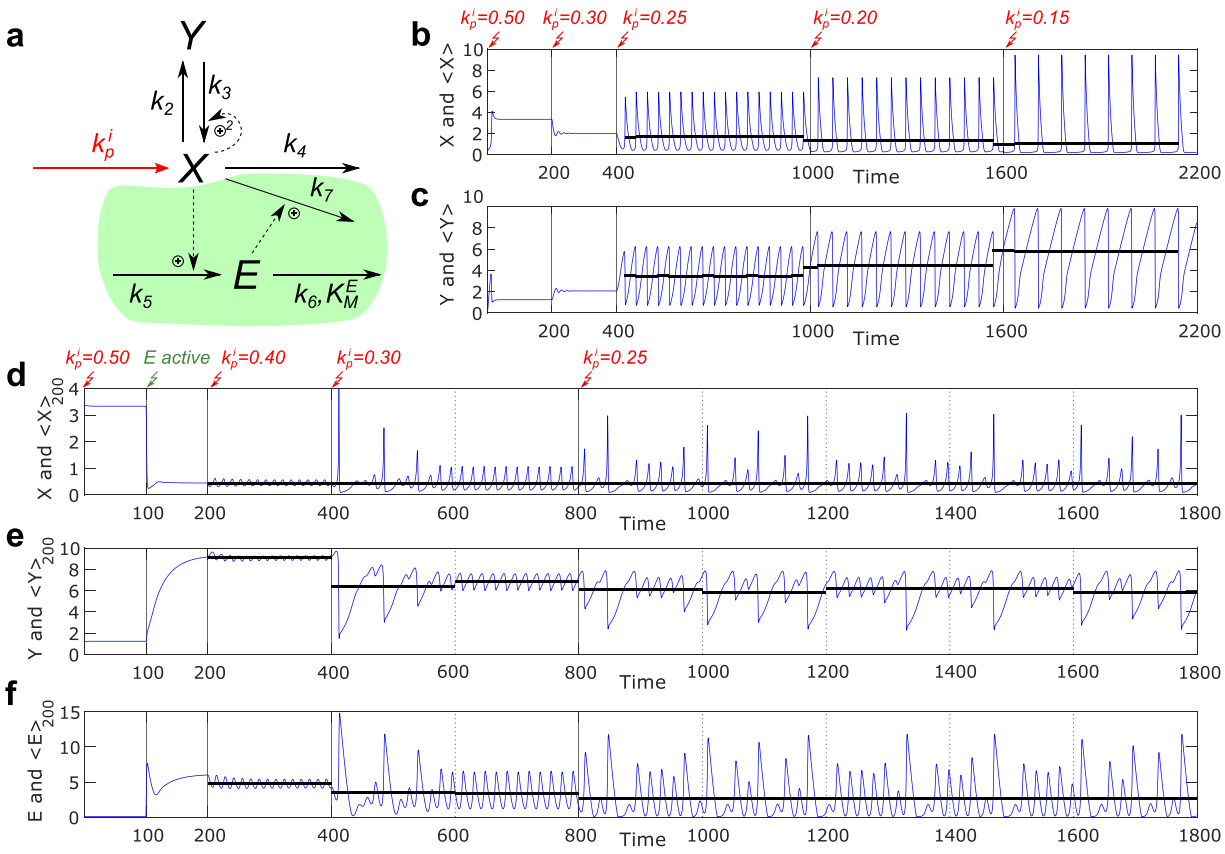

Fig. 7. Behavior of the Brusselator with and without added integral control. (a) Brusselator (white background) and an added outflow controller motif (green background) that provides integral control of X. The system behavior will be analyzed for varying production of X, i.e., the k_p^i parameter is treated as a disturbance. (b) and (c) Behavior of the pure Brusselator, Eqs. (22)–(23) (without added integral control). The plots show the concentration of the chemical species X and Y in blue for different values of the disturbance k_p^i. The periodic average is plotted in black when the system oscillates. The disturbance k_p^i is changed from 0.5 to 0.15 in steps at the times indicated in the figure. Parameters: k_2=0.95, k_3=0.23, k_4=0.15. Initial conditions: X_0=Y_0=0.1. (d)–(f) Behavior of the Brusselator with added integral control, Eqs. (25)–(27) (from t=100). The plots show the concentration X, Y, and E in blue, in addition to the average of these variables in black calculated over fixed intervals with a length of τ=200 starting from t=200 to t=400, from t=400 to t=600, and so on. The controller is activated at t=100 by changing the value of parameters k_5 to k_7 from zero to their value listed in the following. The disturbance k_p^i is changed from 0.5 to 0.25 in steps at the times indicated in the figure. Parameters: k_2=0.95, k_3=0.23, k_4=0.15, k_5=2.7, k_6=1.2, k_7=0.16, and $K_M^E = 0.03$. Initial conditions: X_0=3.3, Y_0=1.3, E_0=0.1.

on the parameters in the controller part of the system. The new equilibrium point is (assuming $K_M^E \ll E$):

$$X^* = \frac{k_6}{k_5}, \quad Y^* = \frac{k_2 k_5}{k_3 k_6}, \quad E^* = \frac{k_p^i k_5 - k_4 k_6}{k_6 k_7}. \tag{28}$$

Given the previous results from Sections 3.1 and 3.2 we should now expect that the integral controller does not only hold X at the setpoint for parameters where the equilibrium is stable, but also that it for parameters that cause the system to oscillate (periodic or chaotic) keeps the *average value* of X at the setpoint. Simulation results shown in Fig. 7d to f confirm that this indeed is the case. When the controller is activated (at $t = 100$ in Fig. 7d) the value of X is moved from 3.33 (k_p^i/k_4) to the setpoint of the controller at 0.44 (k_6/k_5). The controller then defends the setpoint as the disturbance k_p^i is changed. The system with integral control starts to oscillate as k_p^i is reduced to 0.4 (at $t = 200$ in Fig. 7d) and to 0.3, but the average level of X is, apart from some transient behavior, kept at the setpoint. This is also the case when the system displays chaotic oscillations, as seen with a k_p^i of 0.25 (from $t = 800$ in Fig. 7d).

The introduction of an integral controller seems to make the solutions of the combined system less stable, or more oscillatory, than for the system without added control. We see that a lesser change in k_p^i is needed to induce oscillations. This makes sense as an integral controller from linear theory is known to reduce the stability margin of a system by causing phase lag. Nevertheless, the integral controller provides a controlling effect during oscillations in that it keeps the average level of A at a defined setpoint independent of disturbances.

4. Discussion

Our results show the ability of integral control, implemented by reaction kinetics, to regulate the average level of a controlled variable in systems showing either periodic or chaotic oscillations.

4.1. The controller motif and integral control

All the examples presented here use the same outflow controller motif (type 5 in [4]). The motif essentially provides a setpoint for the controlled variable, and acts as an integral controller that changes the value of the controller variable E until the controlled variable (A, or X) is equal to the setpoint. A key feature is that the setpoint only depends on parameters related to the kinetics of the controller species E itself; it is independent of the parameters of the surrounding system that the controller controls. This means that if we are able to add a controller motif to an already existing reaction kinetic network, for example by use of gene editing and synthetic biology, we can, at least as far as the practical methods allow, design it to have the setpoint we want [4,8].

What the setpoint really is, and what integral control manifests itself as in the combined process-controller system, is an equilibrium point where the controlled variable has the value

of the setpoint. This is clearly demonstrated by the addition of integral control to the Brusselator in Section 3.3. The equilibrium of X is moved from a point dependent on the parameters of the Brusselator system, k_p^i/k_4 (Eq. (24)), to a point dependent on the parameters of the controller system, k_6/k_5 (Eq. (28)). It is from this easy to understand how integral control in the case when the equilibrium is stable provides setpoint tracking, and disturbance rejection against disturbances in any parameters apart from k_5 and k_6.

However, although adding integral control provides a new (controllable) equilibrium point, there is no guarantee about the reachability and stability of this point. What our results show here is the effect integral control has when the equilibrium point it provides is unstable and enclosed by a limit cycle or a chaotic attractor. Our results show that integral control in this case keeps the average level of the controlled variable equal to the value it has in the unstable equilibrium point (setpoint). Mathematically speaking, if the controlled variable is X then the integral controller fixes the X coordinate position of the attractor in state space. Disturbance rejection for the average level of the controlled variable readily follows, because the value of the controlled variable in the unstable equilibrium point still depends only on the controller parameters (k_5 and k_6).

4.2. Oscillations, chaos, and steady states

Robust control of the average level of a variable can be seen as a generalization of the well known steady state property of integral control, as the average level and the steady state level are overlapping for nonoscillatory systems. The steady state condition, i.e., assuming steady state by setting the derivatives equal to zero, is normally used to derive the property of integral control. This condition cannot be used directly when the system, which the integral controller is a part of, shows oscillatory behavior. Nevertheless, as long as there is an attractor, enclosing the unstable equilibrium point, that attracts and confines the trajectories, the system is still in what we can call a stable regime. The trajectories are not diverging, but bounded with repetitive (although not always exactly predictable) behavior. Seen from its outside borders the attractor behaves just like an asymptotically stable equilibrium point. The conditions we have used in Eqs. (7) and (19) can be viewed as an extension, or replacement, of the steady state condition. The condition in Eq. (7) can be used for systems that show periodic oscillations; and it can also be used for nonoscillatory systems, for which it becomes the same as the ordinary steady state condition. Likewise, the condition in Eq. (19) can be used for chaotic, periodic, and ordinary nonoscillatory systems.

While the ability to robustly defend an average value is exciting, there are some caveats. Disturbances do not change the average value, but they do change the amplitude and frequency of the oscillations. The variation in amplitude is clearly seen in the two bifurcations plots in Fig. 4d and e for the chaotic outflow controller. For example a k_2 of 0.6 and 2.4 both produce simple periodic oscillations with the same average value of A, but with almost a twofold difference in amplitude.

4.3. Biological significance

According to the classical concept by Cannon, homeostasis keeps the concentrations of certain compounds within tolerable limits and thereby contributes to the internal stability of cells and organisms [49]. Our results explain how integral control enables biological systems to maintain robust homeostasis in the average, even when they show periodic or chaotic behavior. In other words it shows that internal regulation against external disturbances (parameter changes) can be maintained even when systems are oscillating. Integral control provides an active regulatory mechanism that extends beyond just the stability of the attractor.

Some may argue that the concepts of chaos and homeostasis appear incompatible even though there are examples of chaotic behavior in biological systems [50–52]. On one hand we have homeostasis as a mechanism to achieve adaptation and stability (and some would argue constancy), while on the other hand chaos is generally associated with processes which look unpredictable and random. In the end the question of whether a chaotic system with internal integral control can be said to be homeostatically regulated is a question of whether to strictly define homeostasis as only constancy. Such a strict definition has before led to new concepts like homeodynamics being introduced to cover the broader range of regulatory behavior [52]. However, instead of dividing it all up, it may be more constructive to generalize and extend the concept of homeostasis to include regulatory networks with oscillatory and chaotic behavior [53].

Oscillatory behavior is, as mentioned in the introduction, quite common in biological systems. One explanation for this is that regulatory networks that provide adaptation and control with very small modifications can be made to show oscillatory behavior. The evolutionary step from an adapting reaction kinetic network to an oscillating one is small. Evolutionary processes may have modified reaction kinetic networks in a way that opens up for oscillations without necessarily having them display this behavior right away. Organisms may then, by further evolution, have evolved signaling mechanisms based on oscillations of regulated compounds.

The step from simple periodic oscillations to chaotic oscillations also seems to be within relatively easy evolutionary reach, as illustrated by the presented reaction kinetic networks. New interconnections and feedbacks are created as organisms evolve to become more complex. Similar to the here presented networks, the presence of multi-looped negative feedbacks has been known to enhance complex and chaotic dynamics [11,54,55]. Our results indicate that such behavior can exist side by side with homeostasis; active regulation by integral control defends homeostasis even under oscillatory and chaotic conditions by keeping the average level under control.

Acknowledgment

This research was financed in part by Program Area Funds from the University of Stavanger, Norway.

Appendix A. Supplementary material

Supplementary text and movies. SM1–SM4: Further studies on the outflow motif, including illustrations of the flow in phase space and reinjection, a movie showing Poincaré sections, first-return maps, and movement of the attractor in phase space. SM5: Averaging over successive intersections of a Poincaré section. SM6–SM7: Study showing the same regulatory effect of integral control, but with a different inflow motif as example. SM8: An example showing control of the average level of A for a motif with spiky chaotic behavior.

Supplementary material related to this article can be found online at https://doi.org/10.1016/j.physd.2019.01.002.

References

[1] T. Yi, Y. Huang, M. Simon, J. Doyle, Robust perfect adaptation in bacterial chemotaxis through integral feedback control, Proc. Natl. Acad. Sci. USA 97 (9) (2000) 4649–4653, http://dx.doi.org/10.1073/pnas.97.9.4649.

[2] J. Stelling, U. Sauer, Z. Szallasi, F.J. Doyle, J.C. Doyle, Robustness of cellular functions, Cell 118 (6) (2004) 675–685, http://dx.doi.org/10.1016/j.cell.2004.09.008.

[3] D. Muzzey, C.A. Gómez-Uribe, J.T. Mettetal, A. van Oudenaarden, A systems-level analysis of perfect adaptation in yeast osmoregulation, Cell 138 (1) (2009) 160–171, http://dx.doi.org/10.1016/j.cell.2009.04.047.
[4] T. Drengstig, I.W. Jolma, X.Y. Ni, K. Thorsen, X.M. Xu, P. Ruoff, A basic set of homeostatic controller motifs, Biophys. J. 103 (9) (2012) 2000–2010, http://dx.doi.org/10.1016/j.bpj.2012.09.033.
[5] D. Del Vecchio, A.J. Dy, Y. Qian, Control theory meets synthetic biology, J. R. Soc. Interface 13 (120) (2016) 20160380, http://dx.doi.org/10.1098/rsif.2016.0380.
[6] Z.F. Tang, D.R. McMillen, Design principles for the analysis and construction of robustly homeostatic biological networks, J. Theoret. Biol. 408 (2016) 274–289, http://dx.doi.org/10.1016/j.jtbi.2016.06.036.
[7] C. Briat, A. Gupta, M. Khammash, Antithetic integral feedback ensures robust perfect adaptation in noisy bimolecular networks, Cell Syst. 2 (1) (2016) 15–26, http://dx.doi.org/10.1016/j.cels.2016.01.004.
[8] J. Ang, D.R. McMillen, Physical constraints on biological integral control design for homeostasis and sensory adaptation, Biophys. J. 104 (2) (2013) 505–515, http://dx.doi.org/10.1016/j.bpj.2012.12.015.
[9] F. Mairet, A biomolecular proportional integral controller based on feedback regulations of protein level and activity, R. Soc. Open Sci. 5 (2) (2018) 171966, http://dx.doi.org/10.1098/rsos.171966.
[10] A. Goldbeter, Computational approaches to cellular rhythms, Nature 420 (6912) (2002) 238–245, http://dx.doi.org/10.1038/nature01259.
[11] B. Novák, J.J. Tyson, Design principles of biochemical oscillators, Nat. Rev. Mol. Cell Biol. 9 (12) (2008) 981–991, http://dx.doi.org/10.1038/nrm2530.
[12] A. Boiteux, A. Goldbeter, B. Hess, Control of oscillating glycolysis of yeast by stochastic, periodic, and steady source of substrate: A model and experimental study, Proc. Natl. Acad. Sci. USA 72 (10) (1975) 3829–3833, http://dx.doi.org/10.1073/pnas.72.10.3829.
[13] P. Richard, The rhythm of yeast, FEMS Microbiol. Rev. 27 (4) (2003) 547–557, http://dx.doi.org/10.1016/S0168-6445(03)00065-2.
[14] J.C. Dunlap, J.J. Loros, Making time: Conservation of biological clocks from fungi to Animals, Microbiol. Spectr. 5 (3) (2017) 1–19, http://dx.doi.org/10.1128/microbiolspec.FUNK-0039-2016.
[15] I. Mihalcescu, W. Hsing, S. Leibler, Resilient circadian oscillator revealed in individual cyanobacteria, Nature 430 (6995) (2004) 81–85, http://dx.doi.org/10.1038/nature02533.
[16] M.B. Elowitz, S. Leibler, A synthetic oscillatory network of transcriptional regulators, Nature 403 (6767) (2000) 335–338, http://dx.doi.org/10.1038/35002125.
[17] J. Hasty, M. Dolnik, V. Rottschäfer, J.J. Collins, Synthetic gene network for entraining and amplifying cellular oscillations, Phys. Rev. Lett. 88 (14) (2002) 148101/1–148101/4, http://dx.doi.org/10.1103/PhysRevLett.88.148101.
[18] J. Stricker, S. Cookson, M.R. Bennett, W.H. Mather, L.S. Tsimring, J. Hasty, A fast, robust and tunable synthetic gene oscillator, Nature 456 (7221) (2008) 516–519, http://dx.doi.org/10.1038/nature07389.
[19] Y. Chen, J.K. Kim, A.J. Hirning, K. Josić, M.R. Bennett, Emergent genetic oscillations in a synthetic microbial consortium, Science 349 (6251) (2015) 986–989, http://dx.doi.org/10.1126/science.aaa3794.
[20] R.J. Field, E. Körös, R.M. Noyes, Oscillations in chemical systems. II. Thorough analysis of temporal oscillation in the bromate-cerium-malonic acid system, J. Am. Chem. Soc. 94 (25) (1972) 8649–8664, http://dx.doi.org/10.1021/ja00780a001.
[21] J.C. Roux, A. Rossi, S. Bachelart, C. Vidal, Experimental observations of complex dynamical behavior during a chemical reaction, Physica D 2 (2) (1981) 395–403, http://dx.doi.org/10.1016/0167-2789(81)90018-X.
[22] A.F. Taylor, M.R. Tinsley, F. Wang, Z. Huang, K. Showalter, Dynamical quorum sensing and synchronization in large populations of chemical oscillators, Science 323 (5914) (2009) 614–617, http://dx.doi.org/10.1126/science.1166253.
[23] A.F. Taylor, M.R. Tinsley, K. Showalter, Insights into collective cell behaviour from populations of coupled chemical oscillators, Phys. Chem. Chem. Phys. 17 (17) (2015) 20047–20055, http://dx.doi.org/10.1039/c5cp01964h.
[24] B. Hess, M. Markus, Order and chaos in biochemistry, Trends Biochem. Sci. 12 (1987) 45–48, http://dx.doi.org/10.1016/0968-0004(87)90024-7.
[25] K.-P. Yip, D. Marsh, N.-H. Holstein-Rathlou, Evidence of low dimensional chaos in renal blood flow control in genetic and experimental hypertension, Physica D 80 (1–2) (1995) 95–104, http://dx.doi.org/10.1016/0167-2789(95)90063-2.
[26] F. Argoul, A. Arneodo, P. Richetti, J.C. Roux, H.L. Swinney, Chemical chaos: from hints to confirmation, Acc. Chem. Res. 20 (12) (1987) 436–442, http://dx.doi.org/10.1021/ar00144a002.
[27] J.C. Roux, R.H. Simoyi, H.L. Swinney, Observation of a strange attractor, Physica D 8 (1–2) (1983) 257–266, http://dx.doi.org/10.1016/0167-2789(83)90323-8.
[28] L.F. Olsen, H. Degn, Chaos in an enzyme reaction, Nature 267 (1977) 177–178, http://dx.doi.org/10.1038/267177a0.
[29] T. Geest, C.G. Steinmetz, R. Larter, L.F. Olsen, Period-doubling bifurcations and chaos in an enzyme reaction, J. Phys. Chem. 96 (14) (1992) 5678–5680, http://dx.doi.org/10.1021/j100193a004.
[30] M. Guevara, L. Glass, A. Shrier, Phase locking, period-doubling bifurcations, and irregular dynamics in periodically stimulated cardiac cells, Science 214 (4527) (1981) 1350–1353, http://dx.doi.org/10.1126/science.7313693.
[31] L.F. Olsen, H. Degn, Chaos in biological systems, Q. Rev. Biophys. 18 (2) (1985) 165–225, http://dx.doi.org/10.1017/S0033583500005175.
[32] M. Markus, D. Kuschmitz, B. Hess, Chaotic dynamics in yeast glycolysis under periodic substrate input flux, FEBS Lett. 172 (2) (1984) 235–238, http://dx.doi.org/10.1016/0014-5793(84)81132-1.
[33] K. Nielsen, P.G. Sørensen, F. Hynne, H.-G. Busse, Sustained oscillations in glycolysis: an experimental and theoretical study of chaotic and complex periodic behavior and of quenching of simple oscillations, Biophys. Chem. 72 (1) (1998) 49–62, http://dx.doi.org/10.1016/S0301-4622(98)00122-7.
[34] J.M. Kembro, S. Cortassa, D. Lloyd, S.J. Sollott, M.A. Aon, Mitochondrial chaotic dynamics: Redox-energetic behavior at the edge of stability, Sci. Rep. 8 (1) (2018) 1–11, http://dx.doi.org/10.1038/s41598-018-33582-w.
[35] K. Thorsen, T. Drengstig, P. Ruoff, Control theoretic properties of physiological controller motifs, in: ICSSE 2013, IEEE International Conference on System Science and Engineering, Budapest, 2013, pp. 165–170, http://dx.doi.org/10.1109/ICSSE.2013.6614653.
[36] T. Drengstig, X.Y. Ni, K. Thorsen, I.W. Jolma, P. Ruoff, Robust adaptation and homeostasis by autocatalysis, J. Phys. Chem. B 116 (18) (2012) 5355–5363, http://dx.doi.org/10.1021/jp3004568.
[37] I. Prigogine, R. Lefever, Symmetry breaking instabilities in dissipative systems. II, J. Chem. Phys. 48 (4) (1968) 1695–1700, http://dx.doi.org/10.1063/1.1668896.
[38] J.J. Tyson, Some further studies of nonlinear oscillations in chemical systems, J. Chem. Phys. 58 (9) (1973) 3919–3930, http://dx.doi.org/10.1063/1.1679748.
[39] K. Thorsen, Controller motifs for homeostatic regulation and their applications in biological systems (Ph.D. thesis), University of Stavanger, 2015.
[40] G.B. Risvoll, K. Thorsen, P. Ruoff, T. Drengstig, Variable setpoint as a relaxing component in physiological control, Physiol. Rep. 5 (17) (2017) e13408, http://dx.doi.org/10.14814/phy2.13408.
[41] K. Thorsen, O. Agafonov, C.H. Selstø, I.W. Jolma, X.Y. Ni, T. Drengstig, P. Ruoff, Robust concentration and frequency control in oscillatory homeostats, PLoS One 9(9) (2014) e107766, http://dx.doi.org/10.1371/journal.pone.0107766.
[42] C. Letellier, E. Roulin, O.E. Rössler, Inequivalent topologies of chaos in simple equations, Chaos Solitons Fractals 28 (2) (2006) 337–360, http://dx.doi.org/10.1016/j.chaos.2005.05.036.
[43] C. Letellier, Chaos in Nature, World Scientific Series on Nonlinear Science, Series A – Vol. 81, World Scientific Publishing Co. Pte. Ltd., Singapore, 2013, p. 378, (Chapter 4).
[44] O.E. Rössler, Chaotic behavior in simple reaction systems, Z. Nat. forsch. A 31 (3–4) (1976) 259–264, http://dx.doi.org/10.1515/zna-1976-3-408.
[45] O.E. Rössler, Chaos in Abstract Kinetics: Two Prototypes, Bull. Math. Biol. 39 (2) (1977) 275–289, http://dx.doi.org/10.1007/BF02462866.
[46] R. Lefever, G. Nicolis, P. Borckmans, The Brusselator: It does oscillate all the same, J. Chem. Soc., Faraday Trans. 1 84 (4) (1988) 1013–1023, http://dx.doi.org/10.1039/F19888401013.
[47] R. Lefever, G. Nicolis, Chemical instabilities and sustained oscillations, J. Theoret. Biol. 30 (2) (1971) 267–284, http://dx.doi.org/10.1016/0022-5193(71)90054-3.
[48] B. Lavenda, G. Nicolis, M. Herschkowitz-Kaufman, Chemical instabilities and relaxation oscillations, J. Theoret. Biol. 32 (2) (1971) 283–292, http://dx.doi.org/10.1016/0022-5193(71)90166-4.
[49] W. Cannon, Organization for physiological homeostatics, Physiol. Rev. 9 (1929) 399–431, http://dx.doi.org/10.1152/physrev.1929.9.3.399.
[50] A.L. Goldberger, Is the normal heartbeat chaotic or homeostatic? Physiology 6 (2) (1991) 87–91, http://dx.doi.org/10.1152/physiologyonline.1991.6.2.87.
[51] T. Elbert, W.J. Ray, Z.J. Kowalik, J.E. Skinner, K.E. Graf, N. Birbaumer, Chaos and physiology: deterministic chaos in excitable cell assemblies, Physiol. Rev. 74 (1) (1994) 1–47, http://dx.doi.org/10.1152/physrev.1994.74.1.1.
[52] D. Lloyd, M. Aon, S. Cortassa, Why homeodynamics, not homeostasis? Sci. World J. 1 (2001) 133–145, http://dx.doi.org/10.1100/tsw.2001.20.
[53] R. Thomas, Laws for the dynamics of regulatory networks, Int. J. Dev. Biol. 42 (3) (1998) 479–485, http://dx.doi.org/10.1387/IJDB.9654035.
[54] L. Glass, A. Beuter, D. Larocque, Time delays, oscillations, and chaos in physiological control systems, Math. Biosci. 90 (1) (1988) 111–125, http://dx.doi.org/10.1016/0025-5564(88)90060-0.
[55] L. Glass, C. Malta, Chaos in multi-looped negative feedback systems, J. Theoret. Biol. 145 (2) (1990) 217–223, http://dx.doi.org/10.1016/S0022-5193(05)80127-4.